Droplet Size Effects on Film Drainage between Droplet and Substrate

Benjamin Steinhaus,† Patrick T. Spicer,‡ and Amy Q. Shen*,†

Mechanical and Aerospace Mechanical Engineering, Washington University in St. Louis, St. Louis, Missouri 63130, and Complex Fluids Group, Procter and Gamble Company, West Chester, Ohio 45069

Received November 18, 2005. In Final Form: March 18, 2006

When a droplet approaches a solid surface, the thin liquid film between the droplet and the surface drains until an instability forms and then ruptures. In this study, we utilize microfluidics to investigate the effects of film thickness on the time to film rupture for water droplets in a flowing continuous phase of silicone oil deposited on solid poly(dimethylsiloxane) (PDMS) surfaces. The water droplets ranged in size from millimeters to micrometers, resulting in estimated values of the film thickness at rupture ranging from 600 nm down to 6 nm. The Stefan−Reynolds equation is used to model film drainage beneath both millimeter- and micrometer-scale droplets. For millimeter-scale droplets, the experimental and analytical film rupture times agree well, whereas large differences are observed for micrometer-scale droplets. We speculate that the differences in the micrometer-scale data result from the increases in the local thin film viscosity due to confinement-induced molecular structure changes in the silicone oil. A modified Stefan−Reynolds equation is used to account for the increased thin film viscosity of the micrometer-scale droplet drainage case.

1. Introduction

The coalescence and deposition of droplets in liquid−liquid systems plays an important role in many industrial processes such as oil separation and petroleum refineries, where the separation of oil droplets from a continuous phase is achieved using plate separators.[1−3] The deposition characteristics of droplets even play an important role in the function of many common household products such as soaps and detergents. With recent advances in biotechnology and nanotechnology, droplet formation and deposition has begun to play an important role in increasingly smaller scales. Droplets ranging in size from hundreds of micrometers down to tens of micrometers are finding applications in protein crystallization[4] and microcultures for cellular studies.[5]

Several parameters including the droplet diameter, interfacial tension, and continuous-phase viscosity have previously been found to play critical roles in droplet deposition and adherence to a surface in a liquid−liquid system. Additionally, several analytical models have been developed that model film drainage. MacKay and Mason[6] used the Stefan−Reynolds equation, applied to the film drainage between two parallel plates, to model the film drainage beneath a droplet approaching a flat surface. They compared the results of this model to experimental data for several different liquid−liquid systems with droplets ranging in diameter from 0.8 to 80 mm. It was found that the accuracy of the Stefan−Reynolds model increased as the droplet diameter decreased. Lin and Slattery[7,8] developed a much more complex hydrodynamic theory for the film drainage that took into account the curvature of the droplet surface over the film. Chen, Hahn, and Slattery[9−11] later extended the film drainage theory to account for the effects of London−van der Waals forces and the electrostatic double layer. The models of Chen and Slattery were then compared to the experimental data collected by MacKay and Mason[6] (along with several other groups) and were found to predict the coalescence times and film thicknesses with greater accuracy than the original Stefan−Reynolds equation. After this work, Frankel and Mysels[12] also formulated an expression directly relating the film thickness under a droplet (Figure 1) to the original droplet radius according to the following equation

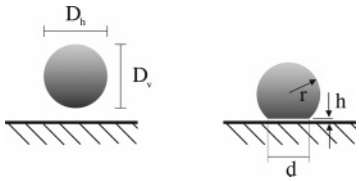

Figure 1. Droplet dimensions.

$$h_o = \sqrt{\frac{0.060 r^5 \rho g \mu_o}{\sigma^2 t}} \quad (1)$$

where h_o is the minimum film thickness at time t, r is the original droplet radius, ρ is the droplet density, μ_o is the film viscosity, σ is the interfacial tension, and g is the gravitational constant. From eq 1, it can be seen that the film thickness at a given time t is a function of the original droplet size. An alternative approach was recently taken by Park, Baldessari, and Leal,[13] who looked at the effects of the thin film molecular weight on droplet coalescence. Their work involved an approach that was distinctly different from those previously mentioned in that it focused on the effects of the critical capillary number (Ca_c) on droplet coalescence. Their findings showed that, for droplets ranging in size from approximately 25−200 μm, there was a direct

* Corresponding author. E-mail: aqshen@me.wustl.edu.
† Washington University in St. Louis, St. Louis.
‡ Procter and Gamble Company.

(1) Rommel, W.; Blass, E.; Meon, W. *Chem. Eng. Sci.* **1992**, *47*, 555.
(2) Rudin, J.; Wasan, D. *AIChE Symp. Ser.* **1980**, *76*, 89.
(3) Wasan, D.; Shah, S.; Chan, M.; Sampath, K.; Sha, R. *ACS Symp. Ser.* **1979**, *91*, 115.
(4) Zheng, B.; Tice, J.; Ismagilov, R. *Anal. Chem.* **2004**, *76*, 4977.
(5) Martin, K.; Henkel, T.; Baier, V.; Grodrian, A.; Schon, T.; Roth, M.; Kohler, J.; Metze, J. *Lab Chip* **2003**, *3*, 202.
(6) MacKay, G.; Mason, S. *Can. J. Chem. Eng.* **1963**, *41*, 203.
(7) Lin, C.; Slattery, J. *AICHE J.* **1982**, *28*, 147.
(8) Lin, C.; Slattery, J. *AICHE J.* **1982**, *28*, 786.
(9) Chen, J.; Slattery, J. *AICHE J.* **1982**, *28*, 955.
(10) Hahn, P.; Chen, J.; Slattery, J. *AICHE J.* **1985**, *31*, 2026.
(11) Chen, J.; Hahn, P.; Slattery, J. *AICHE J.* **1988**, *34*, 140.
(12) Frankel, S.; Mysels, K. it *J. Phys. Chem.* **1962**, *66*, 190.
(13) Park, C.; Baldessari, F.; Leal, L. *J. Rheol.* **2003**, *47*, 911.

10.1021/la0531300 CCC: $33.50
Published on Web 05/06/2006

Table 1. Liquids Used in the Deposition Study

dispersed phase liquid	continuous phase liquid	viscosity ratio λ	interfacial tension σ (mN/m)	density difference $\Delta\rho$ (kg/m^3)
water	200 cSt oil	0.005	30	100
27% glycerol/73% water	200 cSt oil	0.010	27	140
water	20 cSt oil	0.050	30	100
water	10 cSt oil	0.100	30	100
27% glycerol/73% water	10 cSt oil	0.200	27	140

relationship between Ca_c and the time to coalescence but very little dependence based on the molecular weight of the continuous phase.

The above film drainage models all showed reasonable agreement with experimental data down to droplet sizes of several hundred micrometers or just below 1 mm. Additionally, Park et al.[13] was able to find good correlations between the value of Ca_c for a system and the time to coalescence for droplet sizes down to 25 μm. In this study, we plan to focus on the Stefan−Reynolds equation and extend it below previous droplet sizes to examine the deposition of droplets whose diameters are less than 10 μm, where the film thickness at rupture was calculated to be less than 10 nm. We also extend the original gravity-driven Stefan−Reynolds equation to take into account situations where viscous drag, not gravity, is the driving force behind the film drainage. A comparison of the experimental data to theoretical values based on the Stefan−Reynolds equation demonstrates that the continuous-phase viscosity increases greatly beneath the small micrometer-scale droplets because of confinement-induced changes in the molecular structure of the silicone oil. This finding confirms the results previously reported by several other groups for the tribology of thin fluid layers.[14−17]

2. Materials and Methods

2.1. Materials. Silicone oils of varying viscosity were used as the continuous-phase fluid in each of these studies. Deionized water and 27% glycerol/73% deionized water (Table 1) were used as the dispersed phases to achieve the desired viscosity ratios, λ, defined as

$$\lambda = \frac{\mu_i}{\mu_o} \tag{2}$$

where μ_i is the droplet viscosity.

2.2. Millimeter-Scale Experimental Setup. A 1 L glass container, having a flat face, was used to hold the continuous-phase liquid. Millimeter-sized droplets were manually generated using a standard syringe fitted with a 24 G needle tip. Individual 5 cm × 2 cm pieces of poly(dimethylsiloxane) or PDMS were cut from the same large 12 cm × 23 cm slab to minimize differences due to polymer inhomogeneities. The individual slabs were attached to a spatula, bent at a 90° angle, which was then lowered into the continuous phase (Figure 2a).

The motion of the droplets was filmed using a Q-Cam CCD camera, fitted with a Nikkor Micro-Lens, at a rate of 2 frames/s (fps). Prior to use, the PDMS surfaces properties were altered from hydrophobic to hydrophilic[18] by plasma treatment in a Harrick Scientific plasma chamber. Hydrophilic PDMS was used because the droplet's collapse onto the surface is more dramatic when the PDMS is hydrophilic as opposed to when it is hydrophobic, greatly reducing errors in measuring the exact time at which the film ruptures (Figure 3). The PDMS slabs were treated for 60 s at 300 mTorr and a medium voltage setting. Prior to plasma treatment, the contact angle for water on PDMS in silicone oil was measured to be 157°; after treatment it was found to be 40°. After treatment, the slabs were immediately used for study.

2.3. Micrometer-Scale Experimental Setup. Using standard soft-lithography techniques, we generated microfluidic geometry to produce and deposit droplets on the micrometer scale. The geometry contained two distinct regions, an upstream region used to generate the droplets[19] and a downstream region used to study the deposition of the droplets (Figure 2b). In the droplet-forming region, the dispersed phase is pumped through the center channel while the continuous phase is pumped through the two outer channels. Shortly after the three fluid streams converge, they are forced through a small 50 μm orifice that breaks the center channel flow apart into droplets. The deposition region consists of four flat PDMS targets immediately downstream of throats or contractions with widths of 500, 250, 100, and 50 μm. In many cases, the large-scale droplets generated by the orifice were broken apart into smaller satellite droplets (ranging in size from 30 μm down to 3 μm) while passing through the deposition region. The majority of our microfluidic data comes, in fact, from the deposition of these satellite droplets. The deposition of these droplets was filmed using a Photron high-speed camera system at frame rates of up to 1000 fps. The generation of hydrophilic PDMS surfaces was achieved through treating the

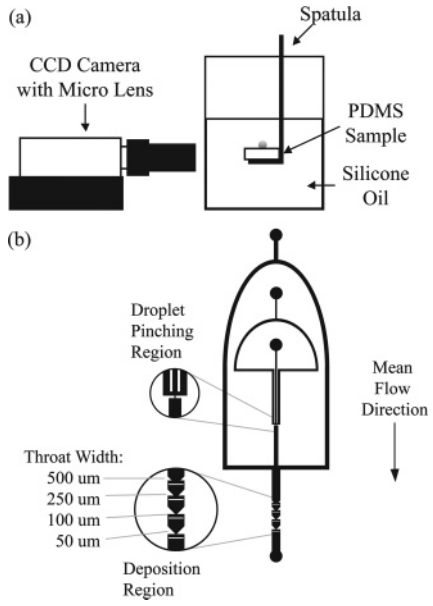

Figure 2. (a) Millimeter droplet deposition setup. (b) Micrometer-sized droplet deposition setup using microfluidic geometry (with gravity perpendicular to and into the page).

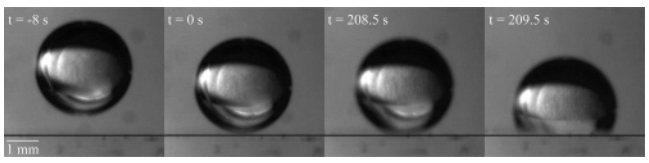

Figure 3. Millimeter-scale water droplet on hydrophilic PDMS immersed in 200 cSt silicone oil (horizon darkened for clarity). The sequence shows the droplet resting on the PDMS surface for over 200 s before the thin film rapidly ruptures.

(14) Hu, Y.; Granick, S. *Tribol. Lett.* **1998**, *5*, 81.
(15) Yamada, S. *Langmuir* **2003**, *19*, 7399.
(16) Luengo, G.; Schmitt, F.; Hill, R.; Israelachvili, J. *Macromolecules* **1997**, *30*, 2482.
(17) Yamada, S.; Nakamura, G.; Amiya, T. *Langmuir* **2001**, *17*, 1693.
(18) Hillborg, H.; Ankner, J.; Gedde, U.; Smith, G.; Yasuda, H.; Wikstrom, K. *Polymer* **2000**, *41*, 6851.

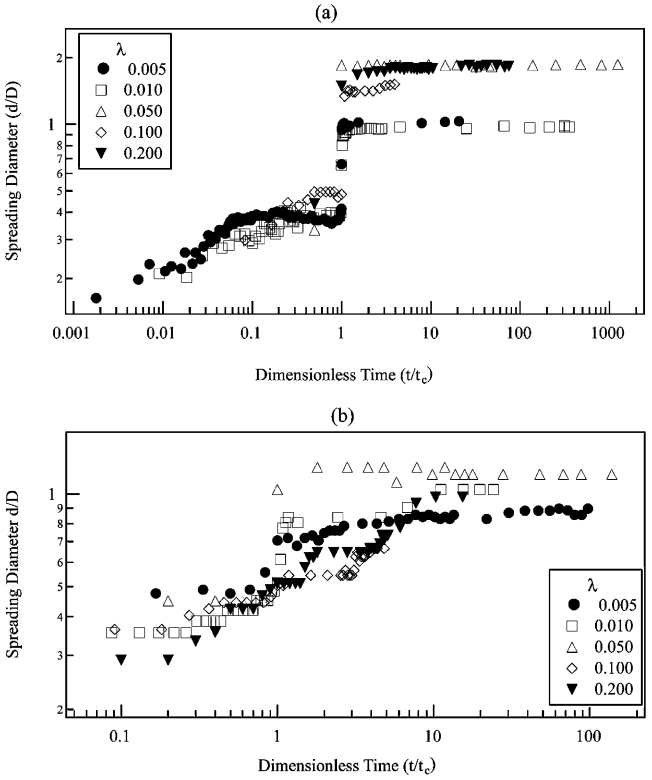

Figure 4. (a) Plot of the spreading diameter (d/D) vs dimensionless time (t/t_c) for the gravity-driven, millimeter-scale droplets. (b) Plot of the spreading diameter (d/D) vs dimensionless time (t/t_c) for the flow-driven, micrometer-scale droplets.

channels under the same plasma chamber setting used in the macroscale studies.

2.4. Video Analysis. Video footage was analyzed using Photron motion analysis software. For each deposition trial, the diameter of the droplet was measured and averaged over the final three frames prior to impact with the target. Droplets were not completely spherical because of viscous drag brought on by their motion through the continuous-phase liquid. The equivalent diameter,[20] D, was used instead and was calculated using $D = (D_h^2 D_v)^{1/3}$, where D_h is the horizontal diameter and D_v is the vertical diameter (Figure 1). Typically, differences between D_h and D_v were less than 5%. The continuous-phase fluid velocity in the region of the droplet impact was assumed to be approximately equal to the droplet's velocity immediately prior to impact. Values of impact velocity were calculated from distance measurements of the center of the droplet and preset time delays between three subsequent exposures immediately prior to impact. After impact, the area of the droplet in contact with the surface was measured and used to find the dimensionless spreading diameter defined as d/D where d is the diameter of the droplet in contact with the surface. The time to film rupture, t_c, was defined as the time elapsed from the point when the droplet began resting on the surface until the point at which the thin film was considered to have ruptured. Film rupture was considered to have occurred when d/D became greater than 0.50.

Because of the fact that the spreading diameter of the droplet increases by such a large amount at a rapid speed once the film had ruptured on top of the hydrophilic PDMS, errors in pinpointing the exact time to film rupture were considered to be relatively small. (See the jump in the curve in Figures 3 and 4.) The accuracy of measuring the film rupture times was primarily limited by the frame rate of the video, which, excluding the most rapid value of t_c, corresponds to errors of no greater than 10%. It should also be noted that the film rupture and resulting collapse of the droplet on the PDMS surfaces is an inherently nonlinear process and as such does not have a high degree of reproducibility. However, future measurements under similar conditions would all be well within an order of magnitude of the values given in this article.

3. Experimental Results

Figure 4 shows the results of a single droplet impact for each of the viscosity ratio systems used in this study on both the millimeter-scale and micrometer-scale data. The majority of the microfluidic data comes from droplets depositing on targets downstream of the 50 and 100 μm throats. In each of these Figures, d/D has been plotted as a function of t/t_c to nondimensionalize and collapse the data. Because of the continual fluid flow in the microchannels, residence times of the micrometer-scale droplets on the PDMS surfaces were much lower than for the millimeter-scale droplets. The end result is that the values of t/t_c do not extend as far to the right in Figure 4b as they do in Figure 4a. The data points past $t = t_c$ are considered to be, for the most part, extraneous because we are interested only in the film drainage beneath the droplet and not the behavior of the droplet after the film has ruptured.

From Figure 4a, it can be seen that the data for each viscosity ratio collapse rather well onto one curve. The only differences arise in the final droplet diameter. For the higher-viscosity ratio systems, the final spreading diameter appears to be much larger than for the lower-viscosity ratio systems.

The data taken from the microfluidic system, in general, show the same initial trend of a constant initial diameter followed by a rapid rise in d/D as the thin film ruptures. One difference to note between parts a and b of Figure 4 is that in the microfluidic system there is much less variance in the final value of d/D, which appears to be much lower than in the millimeter-scale system.

4. Analytical Modeling

To calculate the rate of film thinning and time to film rupture, we employ the Stefan−Reynolds equation used by MacKay and Mason,[6] which models the droplet and surface as two parallel disks being pushed together with a force F

$$-\frac{dh}{dt} = \frac{2Fh^3}{3\pi\mu_o c^4} \tag{3}$$

where h is the film thickness and c is the disk radius. Deryaguin[21] originally derived an expression for c based on a balance between the capillary and buoyancy or gravity forces acting on a droplet resting on a surface such that

$$\pi c_g^2 \frac{2\sigma}{r} = \frac{4}{3}\pi r^3(\Delta\rho)g \tag{4}$$

Solving for c_g then yields

$$c_g = r^2\sqrt{\frac{2(\Delta\rho)g}{3\sigma}} \tag{5}$$

For the microfluidic system, the drag force generated by the flow of the continuous-phase fluid becomes the driving force. For simplicity, this force has been modeled as the viscous drag on a sphere so that the force balance becomes

$$\pi c_v^2 \frac{2\sigma}{r} = 6\pi r\mu_o v \tag{6}$$

$$c_v = r\sqrt{\frac{3\mu_o v}{\sigma}} \tag{7}$$

where v is the continuous-phase fluid velocity. Substituting these values of c back into the original equation for dh/dt along with the corresponding buoyancy or viscous drag forces for F yields

$$-\frac{dh_g}{dt} = \frac{2\sigma^2}{\mu_o(\Delta\rho)gr^5}h_g^3 \quad (8)$$

$$-\frac{dh_v}{dt} = \frac{4\sigma^2}{9\mu_o^2 vr^3}h_v^3 \quad (9)$$

To solve eqs 7 and 8, we impose boundary conditions of an initial and a final film thickness. The initial film thickness was estimated to be $^1/_{10}$ the original droplet radius. It should be noted at this point that the initial film thickness was found numerically to have no effect on the time to rupture, even after varying over several orders of magnitude. The interstitial film shows an initial exponential decay making the final time to coalescence virtually independent of h_o (Figure 6).

The final film thickness was estimated by using the expressions of Chen, Hahn, and Slattery.[22] Their analysis is based on a hydrodynamic theory of the thin film drainage and includes the effects of dimpling and deformation of the droplet surface as well as the effects of London−van der Waals forces on film drainage. Using the results of their linear stability analysis we find

$$h_{fg} = 1.018\left(\frac{Bc^2}{\sigma}\right)^{1/5} \quad (10)$$

$$h_{fv} = 0.802\left(\frac{Bc^2}{\sigma}\right)^{1/4} \quad (11)$$

where B is the Hamaker constant and is estimated to be 10^{-19} erg·cm.

Rupture times were then calculated by time stepping through the expressions for dh/dt from h_o to h_f. Using this process, two values of t_c were calculated for each viscosity ratio—one for the millimeter-scale droplets and one for the micrometer-scale droplets.

In addition to the above, a third set of rupture times was also calculated for the microfluidic system, modeling possible changes in the film's effective interstitial film viscosity as the thickness thins below 10 nm in the microfluidic system. It has recently been shown that liquids confined between solid boundaries that are separated by a few molecular diameters exhibit increased viscosities.[14−17,23,25−27,30] For example, Van Alsten and Granick[26] observed increases in effective viscosity for silicone oil films up to 10 nm thick. For our micrometer-size droplet systems, all of the final film thickness (with the exception of $\lambda = 0.005$) are less than 10 nm. Even though the molecules in these thin films may not enter into a highly ordered state because of confinement-induced changes in the molecular structure of the silicone oil, the thin film can still exhibit increases in its effective viscosity. Detailed surface force measurements are needed to verify these molecular configurations in future work. Here, we estimate the changes in effective viscosity by performing an exponential curve fitting on the data of Van Alsten and Granick,[26] who measured changes in the viscosity of silicone oil, with a molecular weight of 1670 g/mol, between sheets of mica as the film thickness decreases down to 4.6 nm. We believe that these data provide a fairly reasonable estimate of the behavior of our silicone oils, particularly with respect to the 10 and 20 cSt silicone oils whose molecular weights (1200 and 2000 g/mol, respectively) are somewhat similar. From these data, we obtain the following expression for the effective viscosity, μ_e

$$\mu_e = 3 \times 10^6 e^{-10^9 h}\mu_o \quad (12)$$

where μ_e is in Pa·s and h is in meters. Rupture times for the microfluidic system were again calculated by time stepping through the expressions for dh/dt from h_o to h_f, with a new effective viscosity calculated at each time step for the modified rupture time of the microfluidic system.

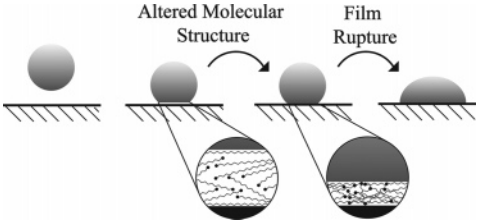

Figure 5. Schematic sequence of the deposition process of micrometer-sized droplets. Because of altered molecular structures in the thin film region, the effective viscosity of the thin film can increase dramatically.

Figure 6 shows the results of the microfluidic simulations for the highest and lowest viscosity ratio systems, $\lambda = 0.200$ and 0.005. We observe that the increases in effective film viscosity have the strong effect of increasing the film rupture time. As the thin film becomes more viscous at smaller thicknesses, it takes longer to drain. This increased drainage time is evident at the right end of the curves because it takes longer for final film thickness h_f to be reached.

It is also worth noting that although we believe the curve fitting performed on the data of Van Alsten and Granick provides a reasonable estimate of the thin film's behavior, eq 12 may slightly underestimate the viscosity increases. The experimental timescale for the data of Van Alsten and Granick was on the order of seconds, and our experimental timescale for the micrometer-scale droplets was on the order of milliseconds. Studies have shown that the timescale over which the film is thinning can effect the thickness at which viscosity increases occur.[27] However, we do not believe that these effects are large enough to create significant errors in our final results.

5. Results and Discussion

For the millimeter-scale droplets, we collected data for five viscosity ratios, λ, ranging from 0.005 to 0.200 on plasma-treated PDMS surfaces. Exposure to plasma gas created a layer of negative hydroxyl groups along the surface of the PDMS, rendering it hydrophilic. In the second set of data, the same fluids and viscosity ratios were used to generate droplets in the microfluidic network. These droplets were then filmed impacting hydrophilic PDMS targets inside the microchannels.

The measured film rupture time (t_c) was then plotted versus the viscosity ratios (λ), along with theoretical values obtained from the Stefan−Reynolds equation (Figure 7). As can be seen, for the macroscale system the values generated by the Stefan−Reynolds equation match the experimental results within an order of magnitude, which is within expectations. However, for the micrometer-sized droplets, the experimentally measured rupture

(19) Anna S. L.; Bontoux N.; Stone H. A. *Appl. Phys. Lett.* **2003**, *82*, 364.
(20) Sikalo, S.; Marengo, M.; Tropea, C.; Ganic, E. *Therm. Fluid Sci.* **2002**, *25*, 503.
(21) Derjaguin, B.; Kussakov, M. *Acta Physiochim. URSS* **1939**, *10*, 25.
(22) Chen, J.; Hahn, P.; Slattery, J. *AICHE J.* **1984**, *30*, 622.
(23) Granick, S. *Science* **1991**, *253*, 1374.
(24) Degennes, P. G. *Adv. Colloid Interface Sci.* **1987**, *27*, 189.
(25) Bhushan, B.; Israelachvili, J.; Landman, U. *Nature (London)* **1995**, *374*, 607.
(26) Van Alsten, J.; Granick, S. *Macromolecules* **1990**, *23*, 4856.
(27) Horn, R.; Hirz, S.; Hadziioannu, G.; Frank, C.; Catala, J. *J. Chem. Phys.* **1989**, *90*, 6767.

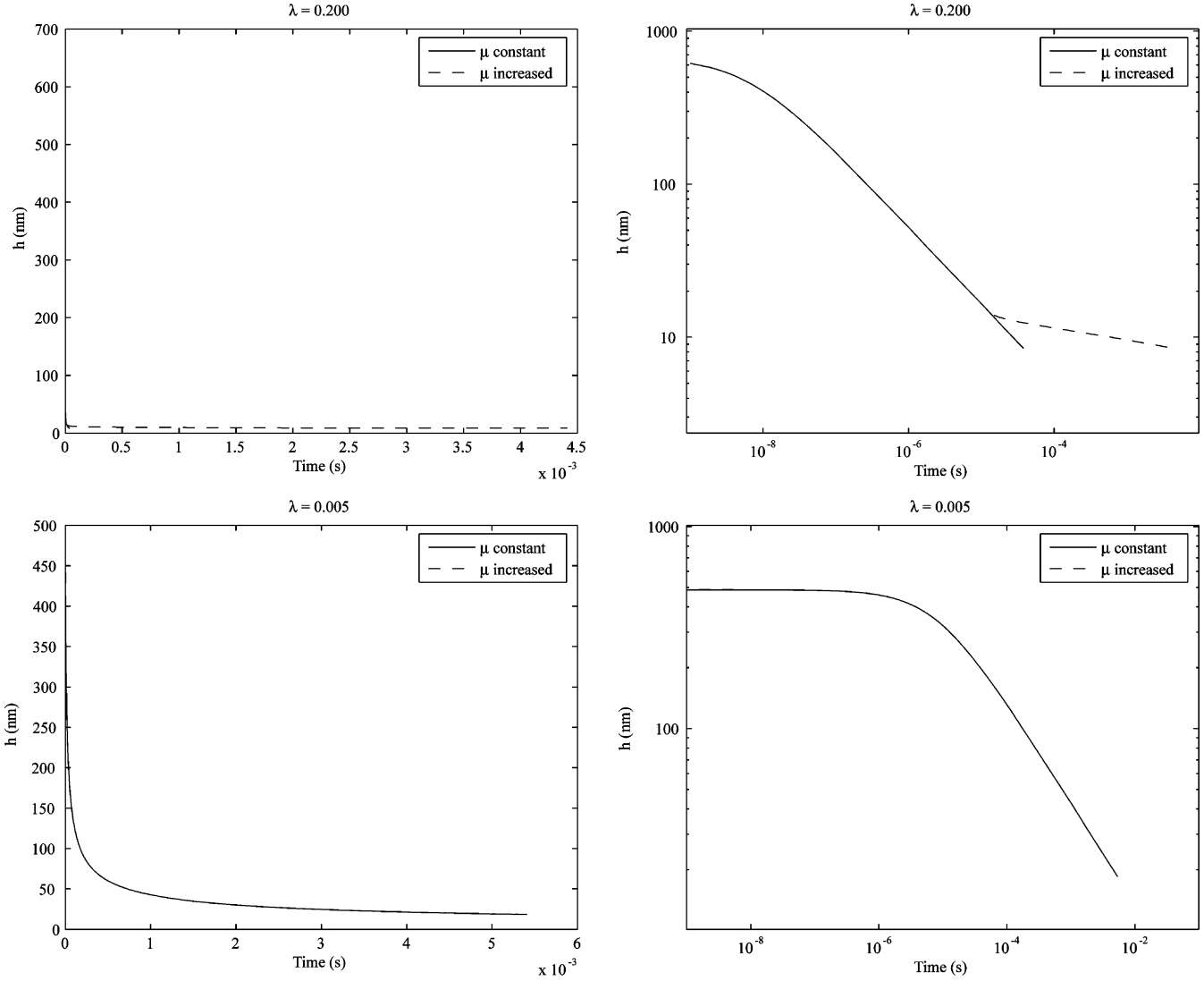

Figure 6. Linear (left) and log−log (right) plots of the analytical results for the Stefan−Reynold's model for the largest and smallest viscosity ratio systems showing differences in the rate of film thinning with and without adjustments to the continuous-phase viscosity.

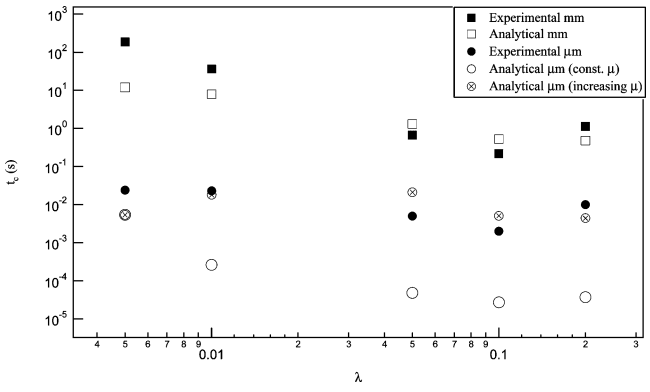

Figure 7. Plot of the time to film rupture (t_c) vs the viscosity ratio.

times are consistently higher than those predicted by the Stefan−Reynolds equation by 2 to 3 orders of magnitude. Once an adjustment has been made to the analytical values to take into account increases in the film viscosity at small thicknesses, the results match those measured experimentally fairly well.

The increase in the shear viscosity of the thin film comes about because of the extremely small dimensions it attains underneath the micrometer-sized droplets. On the basis of the analysis of Chen, Hahn, and Slattery,[21] the thickness of the silicone oil film at rupture, where viscosity increases are expected to occur, will be on the order of 6 to 8.7 nm, which corresponds to 9 to 14 layers of silicone oil based on the molecular width of the silicone oil.[28] Recent work looking at the effects of long-range forces on the deformation of droplets during coalescence has predicted nearly identical film thicknesses at which the droplet will jump and coalesce to the adjacent surface.[29] At these small length scales, the shear viscosity of the thin film can increase dramatically. We offer two possible explanations for these changes in the thin film viscosity. Viscosity increases may be brought on from the entropic penalty of confining the polymer chains within a narrow gap. According to free volume concepts, the fraction of molecular free volume decreases along with the thickness constraints. As the film thickness decreases, fewer and fewer conformations are available for the polymer chains. As the polymer chains become increasingly restricted, they may begin to overlap, leading to increased steric repulsion and a larger effective viscosity in the thin film. An alternative explanation may come simply from the polydispersity of the silicone oil. Although not measured specifically in this experiment, all silicone oils contain chains of several different lengths. It may be that the shortest chains are being squeezed out of the film first. The

(28) Sun, G.; Kappl, M.; Pakula, T.; Kremer, K.; Butt, H. J. *Langmuir* **2004**, *20*, 8030.

(29) Chen, N.; Kuhl, T.; Tadmor, R.; Lin, Q.; Israelachvili, J. *J. Phys. Rev. Lett.* **2004**, *92*, 024501.

end result would be a thin film with longer-chain molecules and hence a viscosity that is larger than the bulk value. Entropy favors smaller molecules in the gap between the droplet and the surface. However, because of the short timescale on which our experiments are occurring, our system is likely not at equilibrium. We should note that although the removal of the shorter silicone oil chains remains a possibility, because of the size of the viscosity increases, it appears less likely than the former explanation.

In either case, these changes can drastically increase the shear viscosity, delaying the thinning of the film and increasing the film rupture time. The end result is a large disparity between the results of the unaltered Stefan−Reynolds model and the experimental values. Further evidence of this behavior can be seen from examining parts a and b Figure 4. In part a of the millimeter-sized droplets, it is the lowest viscosity ratio systems that have the lowest values of d/D after film rupture, on the order of about 1. For the micrometer-sized droplet data in part b, nearly all of the values of d/D are 1 or below, denoting a high interstitial film effective viscosity. However, detailed surface force measurements are needed to verify the molecular configurations and the local viscosity of the silicone thin film.

It should also be noted that the Stefan−Reynolds equation is meant to apply to drainage between two rigid disks. In this study, only one of the interfaces, the solid PDMS surface, is rigid. The droplet surface may in fact undergo a significant amount of deformation while impacting the surface.[30] However, we believe that this will have a minimal effect on the results of our analytical model. In general, the Stefan−Reynolds equation overpredicts the time to coalescence within a 50% error.[6] A majority of the unadjusted micrometer-scale coalescence times are 2 to 3 orders of magnitude smaller than those measured experimentally. More importantly, although the Stefan−Reynolds equation was used to model the fluid flow, our final film thickness has been calculated using the expression described by Chen and Slattery,[9] which takes into account the dimpling of the droplet as it approaches the solid PDMS surface. As can be seen from the millimeter-scale data, the result of combining Chen and Slattery's final film thickness prediction with the Stefan−Reynolds equation yields reasonably accurate results.

(30) Klein, J. *Annu. Rev. Mater. Sci.* **1996**, *26*, 581.

6. Conclusions

The Stefan−Reynolds equation has been extended to model the effects of flow-induced film rupture observed when micrometer-scale droplets deposit on surfaces in a microfluidic geometry. The experimental film rupture times were compared to theoretical predictions based on the Stefan−Reynolds equation for both the millimeter- and micrometer-scale systems. For the millimeter droplet system, the experimental and analytical film rupture times agree well, but large differences are observed in the micrometer-scale droplets system. These differences in the micrometer-scale data can be explained by considering the nanometer thickness of the thin film under the micrometer-sizes droplets and how the local viscosity of these extremely thin films increases as a result of changes in the molecular structure of the thin film. Altering the traditional Stefan−Reynolds equation to take into account the increases in thin film effective viscosity due to the altered molecular structures in the thin films of silicone oils corrects for this discrepancy. Finally, it should be noted that surface forces, thin film dewetting, and possible nucleation at defects can become important at film thickness on the order of nanometer size during film drainage. These above factors have not been studied in this paper and will be investigated in future work.

Acknowledgment. We acknowledge financial support of this work from the North American Technology Council of the Procter and Gamble Company.

LA0531300